

The large coordination number expansion of a lattice Bose gas at finite temperature

Patrick Navez¹, Friedemann Queisser^{2,3} and Ralf Schützhold²

¹ *Department Physics, University of Crete, PO Box 2208, Heraklion 71003, Greece*

² *Fakultät für Physik, Universität Duisburg-Essen, Lotharstrasse 1, 47057 Duisburg, Germany*

³ *Department of Physics, University of British Columbia, Vancouver, V6T 1Z1 Canada*

(Dated: August 24, 2016)

The expansion of the partition function for large coordination number Z is a long standing method and has formerly been used to describe the Ising model at finite temperatures. We extend this approach and study the interacting Bose gas at finite temperatures. An analytical expression for the free energy is derived which is valid for weakly interacting and strongly interacting bosons. The transition line which separates the superfluid phase from Mott insulating/normal gas phase is shown for fillings $\langle \hat{n} \rangle = 1$ and $\langle \hat{n} \rangle = 2$. For unit filling, our findings agree qualitatively with Quantum Monte-Carlo results. Contrary to the well-known mean-field result, the shift of the critical temperature in the weakly interacting regime is apparent.

PACS numbers: 03.75.Hh, 03.75.Kk, 67.85.-d, 05.30.Rt, 05.30.Jp,

I. INTRODUCTION

The Bose-Hubbard model describes interacting bosons in periodic potentials and was originally introduced to study low energy excitations and the solid-superfluid phase transition in ^4He [1–3]. Later on it has been used to describe properties of Josephson junction arrays [4] and ^4He absorbed in porous media [5]. Within the last decade, the Bose-Hubbard model has attracted increasing attention since its experimental realization became possible by means of interacting bosons in optical lattices [6–12]. The system exhibits a Mott insulating and a superfluid phase. The second order phase transition, resulting from the competition between hopping energy and interaction energy, has been observed for bosons in optical lattices [12].

On the theoretical side, the Bose Hubbard Hamiltonian has been studied perturbatively for strong and weak coupling [13–18] and for large and small filling factors [19, 20]. Furthermore, it has been investigated using dynamical mean-field theory [21–25], a slave-boson approach [26], exact diagonalisation [27], Monte Carlo methods [28–30] and the Density Matrix Renormalization Group technique [31–33].

The goal of the present work is to study thermal properties of interacting Bosons using an expansion of the partition function into inverse powers of the coordination number Z , i.e the number of nearest neighbors on a given lattice. The formalism has been previously applied to the Ising model [34–38] where Z was taken to be the number of spins in the range of the exchange potential. It was found that the results are in good agreement with rigorous high-temperature and low-temperature expansions [36]. A related approximation method was previously applied to investigate the dynamics of lattice site correlations after a quantum quench [39–41] and particle-hole pair creation in tilted optical lattices [42]. The $1/Z$ -expansion is valid for all values of the interaction energy and the hopping energy. Therefore, it is suited to study the intermediate regime between the strongly in-

teracting regime on the one hand and the weakly interacting regime on the other hand. In the strongly interacting regime, the (thermal) state of the system respects the $U(1)$ -symmetry of the Hamiltonian and the correlations are short-ranged. If the kinetic term dominates, the $U(1)$ -symmetry is broken and spatial correlations become long-ranged. It should be noted, that the $U(1)$ -phase is divided into a Mott insulating phase and a normal gas phase which are separated by a crossover. This crossover occurs when the typical energy of thermal excitations, $k_B T$, is of the same order as the energy gap of the system. It becomes manifests in the gradually vanishing of the Mott lobes [43–45].

In the following we will focus on the finite temperature phase transition of the Bose-Hubbard system in three dimensions [28, 29, 45–47]. The paper is organized as follows. After reviewing the $1/Z$ -expansion of the partition function for the classical Ising model in section II, we apply it to interacting Bosons in section III and derive various thermodynamic quantities. In section IV, we depict finite temperature phase diagrams which are evaluated from the analytical expressions and compare with results from the literature.

II. THE CLUSTER EXPANSION

We start by reviewing the main arguments of [34, 35] which led to a systematic expansion of the Ising model partition sum into inverse powers of the coordination number Z . The energy of the classical Ising model with a constant interaction strength V within a finite range is given by

$$E = -\frac{1}{2} \frac{V}{Z} \sum_{\mu \neq \nu} T_{\mu\nu} s_\mu s_\nu, \quad (1)$$

where s_μ is a random variable which take the values ± 1 and $T_{\mu\nu}$ is equal to unity inside the interaction range and zero elsewhere.

The Curie point is reached by varying the spin density at fixed interaction strength or by increasing the interaction strength at fixed density. When the number of spins in the interaction range is increased whereas the potential strength is decreased $\sim 1/Z$, the Curie point is fixed. Assuming that only configurations with an average magnetization $R = \sum_{\mu} s_{\mu}/N$ are taken into account, we obtain for $Z \rightarrow N$ the molecular field limit

$$E = \frac{N}{2} V R^2 + \mathcal{O}(1). \quad (2)$$

This limiting procedure motivates the choice of $1/Z$ as a suitable expansion parameter for calculating corrections to the molecular field limit. The corrections are determined by the correlations among different spins. To quantify the correction up to first order $1/Z$, we consider the partition function Ξ and the free energy $\ln \Xi$, respectively.

$$\ln \Xi = \ln \sum_{\{s_{\mu}=\pm 1\}} \exp \left[\frac{\beta V}{2Z} \sum_{\mu \neq \nu} T_{\mu\nu} s_{\mu} s_{\nu} \right] \quad (3)$$

This function can be represented as a sum of connected diagrams and its expansion (3) into powers of β produces

$$\ln \Xi = \sum_n \frac{\beta^n}{n!} M_n, \quad (4)$$

where the M_n 's can be ordered by powers of the expansion parameter $1/Z$. For simplicity, we assume a vanishing magnetization, $R = 0$, such that the leading contribution is of order $1/Z$. Diagrammatically, the lowest order in $1/Z$ can be represented to each order in β by a ring diagram, see Fig. 1.

Other diagrams, for example the ladder diagram in Fig. 1, are of higher order since each solid bond gives an additional factor of $1/Z$. The ring diagrams correspond to the summation over all self-avoiding closed paths on the lattice,

$$M_n^{\text{ring}} = \frac{(n-1)! V^n}{2Z^n} \sum_{\mu_1 \neq \mu_2 \neq \dots \neq \mu_n} T_{\mu_1 \mu_2} T_{\mu_2 \mu_3} \dots T_{\mu_n \mu_1}. \quad (5)$$

Since it is difficult to evaluate the sums for large n , even for nearest-neighbor interaction on a square lattice, we turn to the so-called random-phase approximation. Therefore we include also closed paths which cross two or more lattice sites more than once such that the summations in (5) are unrestricted. This procedure is formally justified since the additional terms, represented by diagram with dashed lines in Fig. 1, are of higher order in $1/Z$. However, it should be noted that this approximation leads to a severe violation of a sum rule $\sum_{\mu} s_{\mu}^2 = N$. Using the Fourier transform given by

$$T_{\mu\nu} = \frac{Z}{N} \sum_{\mathbf{k}} T_{\mathbf{k}} e^{i\mathbf{k} \cdot (\mathbf{x}_{\mu} - \mathbf{x}_{\nu})} \quad (6)$$

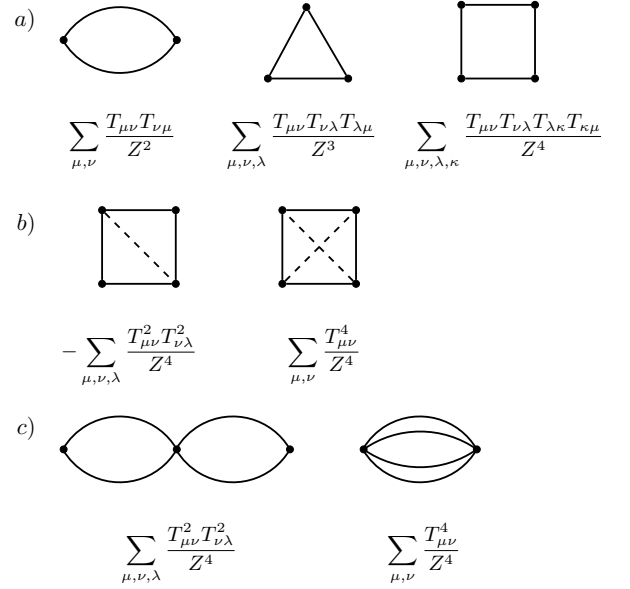


FIG. 1. a) Graphical illustration of the first three geometrical factors of order $1/Z$ in the partition sums of the Ising model (3) and the Bose-Hubbard model (14) up to the 4th order. The lines represent the hopping between the lattice sites whereas the points represent the correlations at a single site. The sums are not restricted such that the Fourier transform can be performed. For this reason, it is necessary to add additional diagrams which are at least of order $1/Z^2$. In b) we depicted the terms which have to be added to the four-vertex expression in a). The dashed lines illustrate the identification of the connected vertices. Each dashed line in a diagram increases the order of the diagram by a factor $1/Z$. c) The geometrical factors of these higher order diagrams are the same as in b) but the correlations functions are different since also four lines meet at a vertex.

we arrive at the expression

$$\begin{aligned} M_n^{\text{ring}} &= \frac{(n-1)! V^n}{2Z^n} \sum_{\mu_1 \dots \mu_n} T_{\mu_1 \mu_2} \dots T_{\mu_n \mu_1} + \mathcal{O}(1/Z^2) \\ &= \frac{(n-1)! V^n}{2} \sum_{\mathbf{k}} T_{\mathbf{k}}^n + \mathcal{O}(1/Z^2). \end{aligned} \quad (7)$$

Summing all the contributions of the ring diagrams, one obtains the free energy

$$\frac{1}{N} \ln \Xi = -\frac{1}{2N} \sum_{\mathbf{k}} \ln[1 - \beta V T_{\mathbf{k}}] + \ln 2 + \mathcal{O}(1/Z^2). \quad (8)$$

From here follows that the correlation length diverges if the temperature approaches the Curie temperature $T_C = 1/V$. A detailed discussion of (8) can be found in [34, 35].

III. BOSE-HUBBARD MODEL

Inspired from the previous section, we use the same expansion technique to analyze the Bose-Hubbard model

up to the first order in $1/Z$. The grand canonical Bose-Hubbard-Hamiltonian has the form

$$\begin{aligned}\hat{H} &= \sum_{\mu} \left[\frac{U}{2} \hat{n}_{\mu}(\hat{n}_{\mu} - 1) - \mu \hat{n}_{\mu} \right] - \frac{J}{Z} \sum_{\mu, \nu} T_{\mu\nu} \hat{b}_{\mu}^{\dagger} \hat{b}_{\nu} \\ &= \sum_{\mu} H_{\mu} + \frac{1}{Z} \sum_{\mu\nu} \hat{H}_{\mu\nu} - \mu \hat{N},\end{aligned}\quad (9)$$

where U denotes the on-site repulsion, J is the hopping rate, and μ the chemical potential. By analogy, we shall consider $T_{\mu\nu} = 1$ for next-neighbors and zero elsewhere renormalized with factor $1/Z$. Switching to the interaction picture, the free energy takes the form

$$\begin{aligned}\ln \Xi &= \ln \text{Tr} \left(e^{-\beta(\sum_{\mu} \hat{H}_{\mu} - \mu \hat{N})} \right. \\ &\quad \times T \left\{ \exp \left[- \int_0^{\beta} d\beta' \frac{1}{Z} \sum_{\mu\nu} \hat{H}_{\mu\nu}(\beta') \right] \right\} \Bigg),\end{aligned}\quad (10)$$

The hopping term depends on imaginary time according to $\hat{H}_{\mu\nu}(\beta) = e^{\beta(\sum_{\mu} \hat{H}_{\mu} - \mu \hat{N})} \hat{H}_{\mu\nu} e^{-\beta(\sum_{\mu} \hat{H}_{\mu} - \mu \hat{N})}$ and $T(\dots)$ denotes the imaginary time ordering operator. As

in field theory, the disconnected diagrams are absent in the logarithm since the free energy is the generating functional of all connected Green's functions [48]. Using the series representation of the exponential, we find

$$\ln \left(\frac{\Xi}{\Xi_0} \right) = \left\langle \sum_{n=1}^{\infty} \frac{(-1)^n}{n! Z^n} T \left(\int_0^{\beta} d\beta' \sum_{\mu\nu} \hat{H}_{\mu\nu}(\beta') \right)^n \right\rangle_{\text{con}} \quad (11)$$

where the brackets in (11) corresponds to the thermal expectation values at $J \rightarrow 0$,

$$\langle \dots \rangle = \frac{\text{Tr} \left(\dots e^{-\beta(\sum_{\mu} \hat{H}_{\mu} - \mu \hat{N})} \right)}{\Xi_0} \quad (12)$$

with the zeroth order partition function

$$\Xi_0 = \left(\sum_{n=0}^{\infty} e^{-\beta[U n(n-1)/2 - \mu n]} \right)^N. \quad (13)$$

The connected parts can be ordered by powers of $1/Z$. In first order only the ring diagrams contribute to the partition function (see Fig.1 and compare with the corresponding expression (5)),

$$\ln \left(\frac{\Xi}{\Xi_0} \right) = \sum_{n=1}^{\infty} \frac{(-1)^n}{n Z^n} \sum_{\mu_1 \neq \mu_2 \dots \neq \mu_n} \int_0^{\beta} d\beta_1 \dots \int_0^{\beta} d\beta_n \left\langle T \left(\hat{H}_{\mu_1 \mu_2}(\beta_1) \hat{H}_{\mu_2 \mu_3}(\beta_2) \dots \hat{H}_{\mu_n \mu_1}(\beta_n) \right) \right\rangle + \mathcal{O}(1/Z^2). \quad (14)$$

Since the summation runs only over pairwise distinct lattice sites, the thermal expectation value can be expressed in terms of the on-site Green functions

$$\begin{aligned}G(\beta_1 - \beta_2) &= \langle T(\hat{b}_{\mu}^{\dagger}(\beta_1) \hat{b}_{\mu}(\beta_2)) \rangle \\ &= \sum_{l=-\infty}^{\infty} e^{2\pi i(\beta_1 - \beta_2)l/\beta} \tilde{G}(i2\pi l/\beta).\end{aligned}\quad (15)$$

Further calculations identify these components as:

$$\begin{aligned}\tilde{G}(i2\pi l/\beta) &= \int_0^{\beta} d\beta' G(\beta') e^{-i\frac{2\pi l\beta'}{\beta}} \\ &= \sum_{n=0}^{\infty} \frac{(n+1)(p_n - p_{n+1})}{2\pi i l/\beta - U n + \mu}\end{aligned}\quad (16)$$

with the p_n being the on-site occupation probabilities in absence of Hopping,

$$p_n = \frac{e^{-\beta(\frac{U}{2}n(n-1) - \mu n)}}{\sum_{m=0}^{\infty} e^{-\beta(\frac{U}{2}m(m-1) - \mu m)}} \quad (17)$$

Again, we apply the random-phase approximation and include terms of order $1/Z^2$ such that the sum over all

lattice sites can be performed. This allows to bring the series into the tractable form

$$\begin{aligned}\ln(\Xi/\Xi_0) &= \sum_{n=1}^{\infty} \sum_{\mu_i} \sum_{l=-\infty}^{\infty} T_{\mu_1 \mu_2} \dots T_{\mu_n \mu_1} \frac{(-J)^n \tilde{G}^n \left(\frac{i2\pi l}{\beta} \right)}{n Z^n} + \mathcal{O} \left(\frac{1}{Z^2} \right) \\ &= - \sum_{\mathbf{k}} \sum_{l=-\infty}^{\infty} \ln \left(1 + J T_{\mathbf{k}} \tilde{G}(i2\pi l/\beta) \right) + \mathcal{O} \left(\frac{1}{Z^2} \right).\end{aligned}\quad (18)$$

Here, the Fourier transform of $T_{\mu\nu}$ has been defined as in (6). The infinite sum over l can be converted to an integral along the real axis according to

$$\begin{aligned}\ln \Xi &= -\beta \sum_{\mathbf{k}} \text{Im} \int_{-\infty}^{\infty} \frac{d\omega}{\pi} \mathcal{P} \frac{\ln(1 + J T_{\mathbf{k}} \tilde{G}(\omega + i0))}{\exp(\beta\omega) - 1} \\ &\quad + N \ln \left(\sum_{n=0}^{\infty} e^{-\beta[U n(n-1)/2 - \mu n]} \right) + \mathcal{O}(1/Z^2),\end{aligned}\quad (19)$$

where the Bose factor has simple poles at $\omega = i2\pi l/\beta$. The compact analytical expression (19) for the free energy of the interacting Bose gas is the main result of our

paper. Since we did not introduce a symmetry breaking parameter in the Hamiltonian, the partition function is valid above the critical temperature for a given ratio J/U . It is valid in the strong interacting regime, $J/U \ll 1$, and gives also the correct limit in the non-interacting limit, $U/J \rightarrow 0$. In particular, we deduce from (19) the partition function of the free Bose-gas,

$$\lim_{U \rightarrow 0} \ln \Xi = - \sum_{\mathbf{k}} \ln (1 - \exp[\beta(\mu + JT_{\mathbf{k}})]) . \quad (20)$$

The on-site probability distribution can be obtained by replacing the potential energy in (19) according $Un(n-1)/2 \rightarrow u_n$ and taking the partial derivative w.r.t. u_n ,

$$\begin{aligned} P_n &= - \frac{1}{\beta N} \frac{\partial}{\partial u_n} \ln \Xi|_{u_n = Un(n-1)/2} \\ &= p_n + \frac{1}{N} \sum_{\mathbf{k}} \sum_{l=-\infty}^{\infty} \frac{JT_{\mathbf{k}}}{1 + JT_{\mathbf{k}} \tilde{G}(i2\pi l/\beta)} \left[p_n \tilde{G}(i2\pi l/\beta) \right. \\ &\quad - \frac{(n+1)p_n}{i2\pi l/\beta - Un + \mu} + \frac{np_n}{i2\pi l/\beta - U(n-1) + \mu} \\ &\quad \left. + \frac{n(p_{n-1} - p_n)/\beta}{(i2\pi l/\beta - U(n-1) + \mu)^2} - \frac{(n+1)(p_n - p_{n+1})/\beta}{(i2\pi l/\beta - Un + \mu)^2} \right]. \end{aligned} \quad (21)$$

From this it is possible to derive an analytical expression for the probability distribution of the free Bose gas which has never been obtained before,

$$\begin{aligned} \lim_{U \rightarrow 0} P_n &= p_n \\ &+ (e^{\beta\mu}(n+1) - n) \frac{p_n}{N} \sum_{\mathbf{k}} \left(\frac{1 - e^{-\beta\mu}}{e^{-\beta(JT_{\mathbf{k}} + \mu)} - 1} + 1 \right). \end{aligned} \quad (22)$$

In Fig. 2, the probability distribution is depicted for various parameters. The filling can be deduced from the partition function Ξ by taking the partial derivative w.r.t. the chemical potential,

$$\begin{aligned} \langle \hat{n} \rangle &= \frac{1}{\beta N} \frac{\partial}{\partial \mu} \ln \Xi = \sum_{n=0}^{\infty} n P_n \\ &= \sum_{n=1}^{\infty} n p_n - \frac{1}{N\beta} \sum_{\mathbf{k}} \sum_{l=-\infty}^{\infty} \frac{JT_{\mathbf{k}} \partial_{\mu} \tilde{G}(i2\pi l/\beta)}{1 + JT_{\mathbf{k}} \tilde{G}(i2\pi l/\beta)}. \end{aligned} \quad (23)$$

The two-point correlations are deduced via the partial derivative w.r.t. the $T_{\mathbf{k}}$

$$\langle \hat{b}_{\mu}^{\dagger} \hat{b}_{\nu} \rangle = \frac{Z}{J} \frac{\partial}{\partial T_{\mu\nu}} \ln \Xi = \frac{Z}{J} \sum_{\mathbf{k}} \frac{\partial T_{\mathbf{k}}}{\partial T_{\mu\nu}} \frac{\partial}{\partial T_{\mathbf{k}}} \ln \Xi, \quad (24)$$

which leads to

$$\begin{aligned} \langle \hat{b}_{\mu}^{\dagger} \hat{b}_{\nu} \rangle &= \frac{i}{2\pi} \lim_{\epsilon \rightarrow 0^+} \int_{-\infty}^{\infty} \frac{d\omega}{e^{\beta\omega} - 1} \frac{1}{N} \sum_{\mathbf{k}} e^{i\mathbf{k} \cdot (\mathbf{x}_{\mu} - \mathbf{x}_{\nu})} \\ &\quad \left(\frac{\tilde{G}(\omega + i\epsilon)}{1 + JT_{\mathbf{k}} \tilde{G}(\omega + i\epsilon)} - \frac{\tilde{G}(\omega - i\epsilon)}{1 + JT_{\mathbf{k}} \tilde{G}(\omega - i\epsilon)} \right) \end{aligned} \quad (25)$$

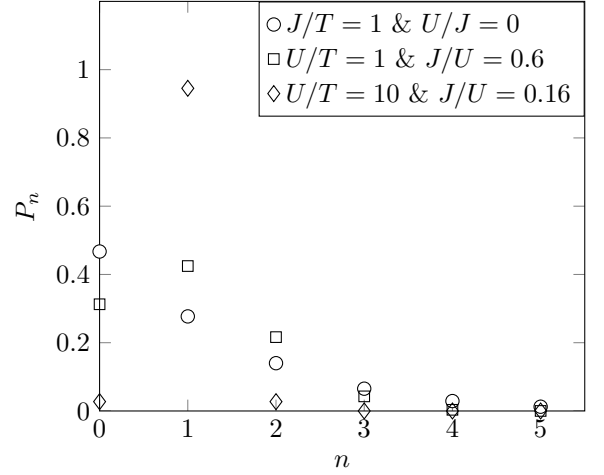


FIG. 2. Probability distribution at unit filling for the free Bose gas (circles) and the interacting Bose gas, (squares and diamonds), see also equations (21) and (22).

Combining the results (23) and (25), we obtain using the Fourier transform the momentum distribution,

$$n_{\mathbf{k}} = \langle \hat{n} \rangle + \sum_{\mathbf{x}_{\mu} \neq \mathbf{x}_{\nu}} e^{i\mathbf{k} \cdot (\mathbf{x}_{\mu} - \mathbf{x}_{\nu})} \langle \hat{b}_{\mu}^{\dagger} \hat{b}_{\nu} \rangle. \quad (26)$$

The partition function (19) can also be used to determine the energy, the specific heat or the entropy of the system.

IV. QUANTUM PHASE TRANSITION

The Bose gas in a lattice resides in the Mott insulating or normal gas phase when the interaction is dominating over the kinetic hopping terms. In this phase, the correlations are short-ranged and the energy spectrum is gapped. When the hopping energy J increases, the correlation length grows and diverges at a critical value J_c . In the following, we use the divergence of the correlation for determining the phase boundary.

To first order in $1/Z$ within the random phase approximation, criterion is equivalent to the divergence of the density distribution $n_{\mathbf{k}}$ at $\mathbf{k} = \mathbf{0}$. This leads to the finite temperature mean-field result [49–51],

$$1 + J_c^{\text{RPA}} \tilde{G}(\omega = 0) = 0. \quad (27)$$

For zero temperature, we obtain from (27)

$$J_c^{\text{RPA}} = U(3 - 2\sqrt{2}) \approx 0.171U. \quad (28)$$

The improvement over the well-known mean-field phase diagrams can be achieved if the dependence of the filling on the parameter J/U is taken into account. Therefore, we calculate the expectation value of the particle number (23) for a given critical temperature and the corresponding critical hopping energy J_c^{RPA} . From the intersections of this curve with $\langle \hat{n} \rangle = 1$ and $\langle \hat{n} \rangle = 2$ at various

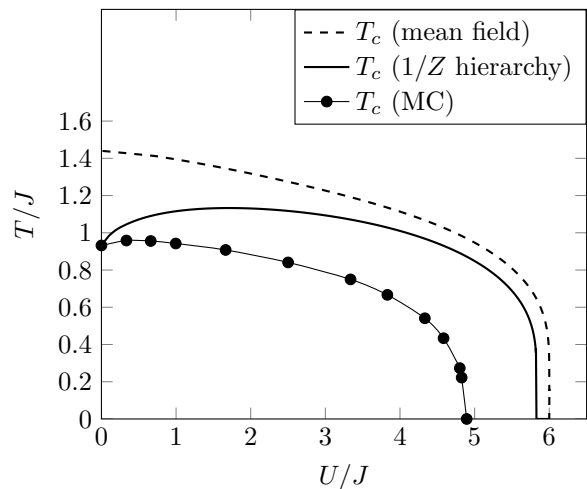


FIG. 3. Phase diagram of the 3D-Bose-Hubbard model for $\langle \hat{n} \rangle = 1$ using the $1/Z$ -results. We compared our results with the mean-field result and with Monte-Carlo-calculations, reproduced from [30]. The phase diagram has been compared with experimental data in [53].

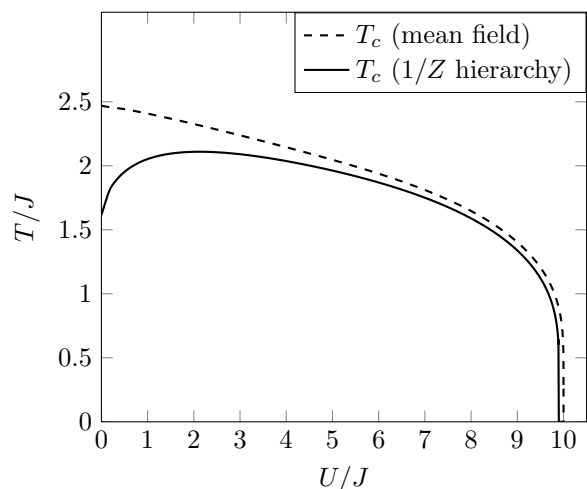


FIG. 4. Phase diagram of the 3D-Bose-Hubbard model for $\langle \hat{n} \rangle = 2$.

temperatures, we can determine the phase boundary at a given filling, see Fig. 3 and Fig. 4. Since the partition function is exact in the limit $J/U \rightarrow \infty$, we arrive at the correct critical temperature for the free Bose gas, $T_c/J \approx 0.93$.

As comparison, we deduced the mean field phase boundary using the particle number probability distribution (17). As can be seen from Fig. 3, the $1/Z$ -method improves qualitatively and quantitatively the phase diagram. First, the correct free Bose-gas limit is approached if the onsite interaction vanishes. Second, there is not discontinuity in the limit $T \rightarrow 0$ as in the mean field approach (see footnote in [52]). It is mainly due to the ran-

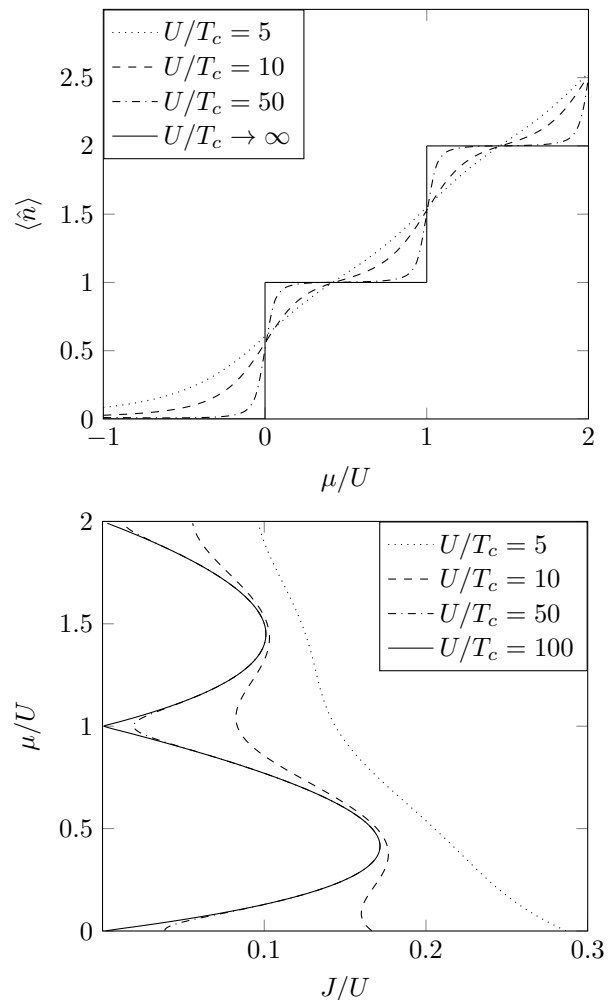


FIG. 5. *Top*: Expectation value of the number operator for different critical temperatures. At each point, the critical hopping is determined by the relation (27). In the limit $T_c \rightarrow 0$, the curves converge to a step-like function where only integer fillings are allowed. The curves soften when the temperature is increased and at $U/T_c \approx 5$ the inflexion points are vanishing. This is the crossover between Mott insulating and normal gas phase [43, 44]. *Bottom*: The solid line encloses the Mott lobes for filling equal to $\langle \hat{n} \rangle = 1$ and $\langle \hat{n} \rangle = 2$ in the limit of vanishing temperature. For increasing temperature, the Mott lobes are vanishing gradually.

dom phase approximation that the results deviate from quasi-exact exact Monte-Carlo simulations [28, 30, 53]. Note that for filling equal to two, the finite temperature phase diagram has not been presented elsewhere.

Fig. 5 (*Top*) shows the filling factor $\langle \hat{n} \rangle$ as a function of μ/U which approaches a staircase function in the limit of vanishing temperature. When the temperature is increased, the plateaus vanish which displays the crossover between Mott insulating phase and normal gas phase [43–45]. The corresponding Mott lobes for different critical temperatures are shown in Fig. 5 (*Bottom*).

V. CONCLUSIONS

We showed that the large coordination number expansion allows a full description of the Bose-Hubbard model at thermal equilibrium in the complete regime from weak to strong interactions. We obtained a closed expression for the partition function of interacting Bosons which is valid for all regimes where the $U(1)$ -symmetry of the model is preserved. From the partition function we obtained local quantities such as the on-site probabilities p_n as well as the non-local thermal correlations $\langle \hat{b}_\mu^\dagger \hat{b}_\nu \rangle$. It should be noted that, in the limit of vanishing tem-

perature, the correlation functions $\langle \hat{b}_\mu^\dagger \hat{b}_\nu \rangle$ as well as the occupation probabilities can also be obtained from $1/Z$ -hierarchy that describes the dynamics of lattice site correlations [39, 42].

ACKNOWLEDGMENTS

PN gratefully acknowledges that this work was supported by the European Union's Seventh Framework Programme (FP7-REGPOT-2012-2013-1) under grant agreement number 316165. Helpful discussions with Konstantin Krutitsky are gratefully acknowledged.

-
- [1] H. A. Gersch, G. C. Knollman, Phys. Rev. **129**, 959 (1963).
 - [2] H. A. Gersch, J. M. Tanner, Phys. Rev. **139**, A1769 (1965).
 - [3] J. F. Fernandez, H. A. Gersch, Phys. Rev. **149**, 154 (1966).
 - [4] L. J. Geerligs, M. Peters, L. E. M. de Groot, A. Verbruggen, and J. E. Mooij, Phys. Rev. Lett. **63**, 326 (1989).
 - [5] M. P. A. Fisher, P. B. Weichman, G. Grinstein, and D. S. Fisher, Phys. Rev. B **40**, 546 (1989).
 - [6] D. Jaksch, C. Bruder, J. I. Cirac, C. W. Gardiner, and P. Zoller, Phys. Rev. Lett. **81**, 3108 (1998).
 - [7] W. Zwerger, J. Opt. B: Quantum Semiclass. Opt **5**, S9 (2003).
 - [8] I. Bloch, Nature Physics, **1**, 23 (2005).
 - [9] C. Sias, A. Zenesini, H. Lignier, S. Wimberger, D. Ciampini, O. Morsch, and E. Arimondo, Phys. Rev. Lett. **98**, 120403 (2007).
 - [10] M. Raizen, C. Salomon, and Q. Niu, Physics Today, **50**, 30 (1997).
 - [11] M. Greiner, O. Mandel, T. Esslinger, T. W. Hänsch, and I. Bloch, Nature **415**, 39 (2002).
 - [12] W. S. Bakr, A. Peng, M. E. Tai, R. Ma, J. Simon, J. I. Gillen, S. Fölling, L. Pollet, and M. Greiner, Science **329**, 547 (2010).
 - [13] J. K. Freericks and H. Monien, Europhys. Lett. **26** 545, (1994).
 - [14] J. K. Freericks and H. Monien, Phys. Rev. B **53**, 2691 (1996).
 - [15] B. Damski and J. Zakrzewski Phys. Rev. A **74**, 043609 (2006).
 - [16] N. Teichmann, D. Hinrichs, M. Holthaus and A. Eckardt, Phys. Rev. B **79** 100503 (2009).
 - [17] K. Sengupta and N. Dupuis, Phys. Rev. A **71**, 033629 (2005).
 - [18] K. Sheshadri, H. R. Krishnamurthy, R. Pandit, and T. V. Ramakrishnan, Europhys. Lett. **22**, 257 (1993).
 - [19] R. Schützhold, M. Uhlmann, Y. Xu and U. R. Fischer, Phys. Rev. Lett. **97**, 200601 (2006).
 - [20] U. R. Fischer, R. Schützhold, M. Uhlmann, Phys. Rev. A **77**, 043615 (2008).
 - [21] A.P. Kampf and G.T. Zimanyi, Phys. Rev. B **47** 279 (1993).
 - [22] L. Amico and V. Penna, Phys. Rev. Lett. **80**, 2189 (1998).
 - [23] A. Hubener, M. Snoek, and W. Hofstetter, Phys. Rev. B **80**, 245109 (2009).
 - [24] Y. Li, M. R. Bakhtiari, L. He, W. Hofstetter, Phys. Rev. B **84**, 144411 (2011)
 - [25] Y. Li, M. R. Bakhtiari, L. He, W. Hofstetter, Phys. Rev. A **85**, 023624 (2012)
 - [26] D. B. M. Dickerscheid, D. van Oosten, P. J. H. Denteneer, and H. T. C. Stoof, Phys. Rev. A **68**, 043623 (2003).
 - [27] K. V. Krutitsky, Phys. Rep. **607**, 1 (2016).
 - [28] B. Capogrosso-Sansone, N. V. Prokof'ev, and B. V. Svistunov, Phys. Rev. B **75**, 134302 (2007).
 - [29] S. Trotzky, L. Pollet, F. Gerbier, U. Schnorrberger, I. Bloch, N. V. Prokofev, B. Svistunov, and M. Troyer, Nat. Phys. **6**, 998 (2010).
 - [30] B. Capogrosso-Sansone, Ş. G. Söyler, N. Prokof'ev, and B. Svistunov, Phys. Rev. A **77**, 015602 (2008).
 - [31] M. Cheneau, P. Barmettler, D. Poletti, M. Endres, P. Schauß, T. Fukuhara, C. Gross, I. Bloch, C. Kollath, and S. Kuhr, Nature **481**, 484 (2012).
 - [32] M. Endres, M. Cheneau, T. Fukuhara, C. Weitenberg, P. Schauß, C. Gross, L. Mazza, M. C. Bañuls, L. Pollet, I. Bloch, S. Kuhr, Science **334** 200 (2011).
 - [33] S. Ejima, H. Fehske, and F. Gebhard, Europhys. Lett. **93**, 30002 (2011).
 - [34] R. Brout, Phys. Rev. A **115**, 824 (1959).
 - [35] R. Brout, Phys. Rev. A **118**, 1009 (1960).
 - [36] G. Horwitz and H. B. Callen, Phys. Rev. **124**, 1757 (1961).
 - [37] R. B. Stinchcombe, J. Phys. C **6**, 2459 (1973).
 - [38] R. B. Stinchcombe, J. Phys. C **6**, 2484 (1973).
 - [39] P. Navez and R. Schützhold, Phys. Rev. A **82**, 063603 (2010).
 - [40] F. Queisser, K. V. Krutitsky, P. Navez, R. Schützhold, Phys. Rev. A **89**, 033616 (2014).
 - [41] K. V. Krutitsky, P. Navez, F. Queisser, R. Schützhold EPJ Quantum Technology **1**, (2014).
 - [42] F. Queisser, P. Navez, and R. Schützhold, Phys. Rev. A **85**, 033625 (2012).
 - [43] B. DeMarco, C. Lannert, S. Vishveshwara, and T.-C. Wei, Phys. Rev. A **71**, 063601 (2005).
 - [44] F. Gerbier, Phys. Rev. Lett. **99**, 120405 (2007).
 - [45] T. P. Polak and T. K. Kopec, J. Phys. B At. Mol. Opt. Phys. **42**, 095302 (2009).
 - [46] Y. Yu and S. T. Chui, Phys. Rev. A **71**, 033608 (2005).

- [47] L. Pollet, C. Kollath, K. Van Houcke, and M. Troyer, New Journal of Physics, **10**, 065001 (2008).
- [48] M. E. Peskin and D. V. Schroeder, An Introduction To Quantum Field Theory, Addison-Wesley (1995).
- [49] P. Buonsante and A. Vezzani, Phys. Rev. A **70**, 033608 (2004).
- [50] K. V. Krutitsky, A. Pelster, and R. Graham, New J. Phys. **8**, 187 (2006).
- [51] S. Fölling, A. Widera, T. Müller, F. Gerbier, and I. Bloch, Phys. Rev. Lett. **97**, 060403 (2006).
- [52] The discontinuity in mean field phase-diagram for $T \rightarrow 0$ has the following origin: The chemical potential is well defined for finite temperatures and one obtains from (17) in the limit $T \rightarrow 0$ the value $\mu/U = 0.5$ for unit filling which corresponds to $U/J_c = 6$. In contrast, the chemical potential is not well-defined within the Mott lobes at $T = 0$. However, it is still possible to deduce the Mott lobe boundaries from (17). For unit filling, the tip of the lobe is at $U/J_c = 3 + 2\sqrt{2}$. This unphysical discontinuity ($\Delta(U/J_c) \approx 0.171$) is not present in the $1/Z$ -approach.
- [53] A.S. Sajna, T.P. Polak, R. Micnas, and P. Rožek, Phys. Rev. A **92**, 013602 (2015).